EFFECT OF WETTING ON PERFORMANCE OF SMALL-SCALE SHEAR WALLS

David T. King

Former Graduate Research Assistant
E-mail: mrdtking@gmail.com

*Arijit Sinha**†

Assistant Professor
E-mail: Arijit.sinha@oregonstate.edu

Jeffrey J. Morrell†

Professor
Department of Wood Science and Engineering
Oregon State University
Corvallis, OR
E-mail: jeff.morrell@oregonstate.edu

Received June 2014

Abstract. Wood shear walls are the main lateral force-resisting system for wood-frame construction. Water intrusion and subsequent decay around connections can significantly impact shear wall behavior, but these problems are seldom studied. In this study, effects of water intrusion and fungal attack on shear wall capacity were examined using small-scale (610- × 610-mm) shear walls that were monitored with time using destructive monotonic tests. Results were compared with tests of dry and water control samples. Although fungal colonization was not successful under the conditions tested, wetting (with or without fungal inoculation) produced interesting effects on shear wall capacity. Wetting alone initially increased shear wall capacity, possibly because of fastener corrosion. Observations and digital image correlation data suggest that tensile forces in the uplift corner of the shear walls governed failure modes, which were primarily nail withdrawal, nail pull-through, flake debonding, and cross-grain tension. Wetting affected rigidity of oriented strandboard and led to more frequent nail pull-through. Although failure loads did not differ between the groups, failure modes and displacement at maximum load suggested decreased performance of wetted shear walls. The results suggest that slight amounts (8% overall) of wetting do not negatively affect shear wall performance. However, the effects of prolonged wetting on capacity merit further study.

Keywords: Durability, lateral force-resisting system, oriented strandboard, moisture intrusion.

INTRODUCTION

Wooden structures must be able to withstand forces from wind and seismic events throughout their lifespan, making lateral resistance an important component in structural design. Most wooden structures use shear walls as the principal lateral force-resisting system for these forces. Shear walls are typically composed of framing lumber and structural sheathing (oriented strandboard [OSB] or plywood) held together with dowel-type fasteners (nails, screws, or staples). Shear walls experience great stress concentrations in the uplift corner during loading (Sinha and Gupta 2009); thus, nailed connections between framing and sheathing members have been determined to be the primary source of strength, stiffness, and energy dissipation in wind and seismic events (Polensek and Bastendorff 1987; Chui et al 1998). Shear walls, like most interior building components, are considered dry-use applications. However, increasingly energy-efficient structures have created changes in building practices that alter moisture levels in structures. Building paper or house wrap is used in

* Corresponding author
† SWST member

conjunction with siding to seal off cracks and create a nearly airtight building envelope. This limits the ability of moisture to enter the building, but problems can occur when interior moisture levels increase to the point at which condensation occurs. Poor construction, roof deterioration, or plumbing problems can lead to additional moisture accumulation that may go unnoticed for months. This trapped moisture creates conditions conducive for fungal attack, which leads to significant structural damage. Although wood composite shear wall behavior has been well documented (McCutcheon 1985; Johnson 1997; Durham et al 2001; van de Lindt 2004; Sinha and Gupta 2009), there is little information on the effects of wetting and fungal decay on shear wall performance.

Kent et al (2004, 2005) found that lateral capacity of connections in OSB in simulated shear wall sections declined at an increasing rate after weight losses exceeded 12%. Nailed OSB connections also experienced significant losses in tensile and compression properties with time when colonized by brown-rot decay (Kent et al 2005). Clearly, water intrusion and subsequent decay around connections can significantly impact shear wall behavior. Interactions between water intrusion and decay around fasteners are a complex problem with multiple interactions that will not be dealt with in this study. This study instead focused on the role of moisture intrusion on shear wall behavior.

Moisture intrusion is a common problem for many structures, and developing data on the impacts of moisture ingress and fungal attack on the behavior of various building elements will help engineers design more resistant structures and evaluate capacity losses in structures that experience wetting. The goal of this study was to better understand the effects of water intrusion and fungal attack on shear wall capacity.

MATERIALS AND METHODS

Assemblies

Shear walls were analyzed using procedures described in ASTM (2012) except that the dimensions were decreased to square frames measuring 610 × 610 mm. The experiment was developed as a completely randomized design with incubation time at five different levels as the primary effect. The shear walls were designed using NDS (2012) guidelines and composed of 38- × 89-mm (nominal 2 × 4) select structural, kiln-dried Douglas-fir lumber and 11-mm-thick Exposure 1 aspen OSB. Each shear wall consisted of 610-mm-long top and bottom plates, two studs (530 mm long), and a 610- × 610-mm OSB panel. Eight 90- × 3.3-mm full round head nails (Senco, Cincinnati, OH) were hand-driven into predrilled 3-mm-diameter holes in the top and bottom plate to assemble the shear wall frame. The OSB (oriented with the strength direction aligned vertically, ie perpendicular to the loading direction) was nailed to the shear wall frame using a pneumatic gun with 60- × 2.9-mm Senco full round head nails at 102-mm spacing, which is common edge spacing in light-frame construction (NDS 2012). This spacing resulted in 24 sheathing nails per panel. Squares of building paper (610 × 610 mm) were fastened to the OSB on the sheathing side of each shear wall with 10- × 3- × 2-mm staples (Duo-Fast, Vernon Hills, IL). Clear polyethylene sheeting was used to cover the open side of each shear wall. The polyethylene sheeting acted as a vapor barrier, restricting evaporation but allowing for observation of the panel interior during incubation. Each sample was weighed after assembly. A total of 112 shear walls were constructed and distributed into the following treatments (Fig 1):

1. Dry controls (eight assemblies) that were tested immediately after construction.
2. Dry controls (eight assemblies) with the lower corner of OSB removed to simulate an assembly in which fungal attack had completely degraded that portion of the OSB.
3. Assemblies (48) that were subjected to wetting only.
4. Assemblies (48) that were subjected to both wetting and fungal inoculation.

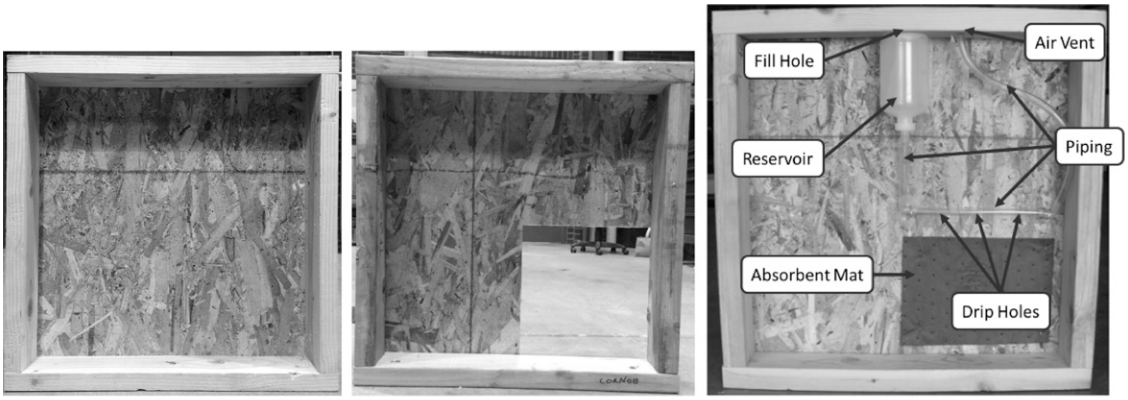

(a) (b) (c)

Figure 1. Shear wall assembly configurations: (a) dry control, (b) no-corner control, and (c) wetting only or wetting and fungal exposure. The wetted assembly (c) also shows the location of the irrigation system.

Uplift Corner

Shear walls are primarily designed to restrain shear, compression, and tensile forces. The location of interest in this study was the uplift corner of the shear wall because this was where large stress concentrations can develop around the connections (Sinha and Gupta 2009). The experimental design focused on wetting and decay development around the uplift corner. An irrigation system was designed to produce a wetting pattern in this part of the shear walls.

The wetting only and wetting–fungal inoculated assemblies were incubated at 30°C and 90% RH. Assemblies were exposed to cyclic wetting using an irrigation system installed within the wall cavity (Fig 1c). Perforated plastic tubing was attached to the uplift corner of the assembly, and a 50-mL reservoir that could be accessed from outside the assembly was placed overhead. A water-absorbent pad was placed on the OSB in the uplift corner to absorb and hold the added water closely to the panel. Every 3 da, 50 mL of water was added to the reservoir for the duration of the experiment to achieve and maintain the target 60% MC (at the uplift corner) as determined by periodic weighing of selected samples. The wetted and wetted–fungal inoculated assemblies were separated from each other to decrease the chance of contamination. Each assembly was inoculated with a brown-rot fungus (*Postia placenta* [Fries] Larsen et Lombard Isolate Madison #698) 9, 26, 31, 70, 76, 83, 122, 129, and 137 da after wetting began using procedures described by Kent et al (2005).

All assemblies were incubated for 32, 112, 177, 234, 258, and 402 da. At the end of each incubation time, eight wetted and eight wetted–fungal inoculated shear walls were removed from the conditioning room. The walls were immediately weighed to determine overall moisture content.

Moisture Content Mapping

Moisture distribution in the uplift corner was determined using a resistance-type moisture meter (Delmhorst Instrument Co., Towaco, NJ) in a grid with 100 or 67 mm between each measurement location. A total of 35 readings were taken per panel. The larger spacing was used in the first three samplings, whereas the closer spacing was used later as it became apparent that more readings were needed to better define the moisture distribution. The moisture meter had a useful range from 5-60% MC with a precision of ±0.25% in the 5-12% MC range and ±1% in the 20-30% MC range. The overall moisture range was useful because it covered the FSP (27-30%) and our target moisture content (60%, oven-dry basis). These data were used to develop moisture content contour plots in SigmaPlot (Systat Software, Inc., San Jose, CA) using a 5 × 7 grid pattern of the inner face of the OSB paneling. These plots were used to categorize wetting patterns on individual shear walls.

Shear Wall Tests

Assemblies were air-dried after moisture content measurements to a target of 12% MC. The dried samples were weighed, and the building paper and polyethylene sheeting were removed. Digital image correlation (DIC) was used as a supplemental part of the testing procedure and required that special steps be taken to prepare the outer OSB surface. The outer side of the OSB paneling of each sample was coated with black paint, and then a paint gun was used to overlay a white speckle pattern on the surface. When the paint was dry, four 13-mm-diameter holes (two in the top plate and two in the bottom plate) were drilled in the shear wall frames and the samples were secured with bolts to a computer-controlled hydraulic-actuated testing device (Fig 2). The loading geometry and test setup incorporated a fixed platform and a kinetic swing arm actuated by a hydraulic ram that induced force on the top plate of each sample. The samples were loaded at a controlled rate of 5 mm/min until failure and a load cell on the hydraulic ram produced force outputs during the loading cycle. A linear variable differential transformer was used to measure relative deflection as each sample was loaded. Some samples exhibited fastener corrosion after exposure. The degree of corrosion was noted, but it was not possible to more closely quantify the degree of corrosion because initial weight and dimension measurements were not available.

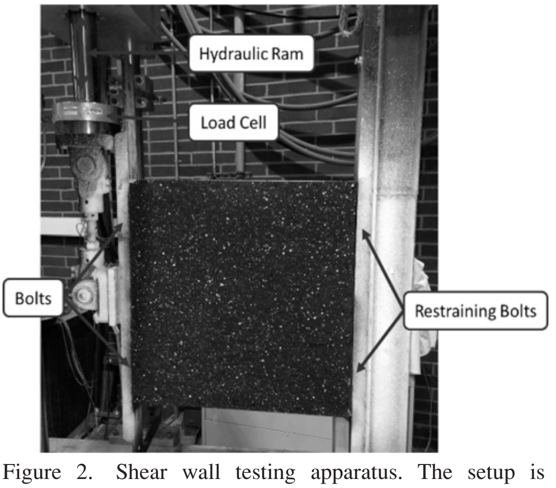

Figure 2. Shear wall testing apparatus. The setup is rotated 90° with the steel channel acting as a foundation.

A noncontact strain measurement system based on the principles of DIC was used to track surface deformation during loading. Two stereo-mounted cameras were focused on the assembly during testing to image the black and white speckle pattern to track speckle movement in space. These cameras first recorded a reference image and then captured a series of images every second during testing. These data were used to create a three-dimensional model of pixel movement with respect to the reference image. An MTS 407 hydraulic controller (MTS Systems Corp., Eden Prairie, MN) was used in conjunction with the DIC software, and each image was tagged with specific load and deflection data. The DIC software uses the images to map the surface of interest by correlating the movement of each pixel to calculate strain. Shear strain (ε_{xy}) is one of many outputs that can be extracted from the acquired data. Shear strain maps were produced from the DIC outputs and used to examine localized strains on each shear wall. Although DIC is only capable of making surface measurements, strain of the OSB was assumed to be representative of strain through the thickness because of strain compatibility.

Statistics

Data were subjected to analysis of variance (ANOVA) ($\alpha = 0.05$), and individual treatments were then compared using unpaired t-tests at $\alpha = 0.05$. Assumptions of the regression, including normality and homogeneity of variance, were evaluated using Tukey's and Levene's tests, respectively (Ramsey and Schafer 2002).

RESULTS AND DISCUSSION

The assemblies tended to wet well during the study, and fungal colonization was erratic. Only two assemblies developed visible fungal attack, and one of these was a noninoculated control. Attempts to isolate *P. placenta* from the remaining assemblies were unsuccessful, and there were no consistent differences in either moisture distribution or shear wall capacity between assemblies that were wetted and those that were wetted and inoculated with the decay fungus. For this reason, the results for these assemblies were combined for discussion. A summary of test results is given in Table 1.

Moisture Content Mapping

Moisture levels in the assemblies, as determined by mass gain, increased by 12-17% overall, but nearly all of this increase occurred in the uplift corners resulting in moisture contents in this region between 52 and 71%. These values closely corresponded to those found using the moisture meter and suggest that the panels were well above the FSP in the uplift zone (Fig 3).

As noted, wetting tended to be concentrated in the uplift corner, reflecting the tendency of the irrigation system to direct water into this region. The bottom of the OSB adjacent to the bottom plate achieved the highest moisture levels, but there were some variations in wetting patterns (Fig 3). Six different wetting patterns occurred (Fig 3) and were arbitrarily called type 1 to type 6. These differences appeared to be caused by the degree of connection between the irrigation system and the panel. Eleven of 96 panels subjected to wetting had very low moisture levels in the uplift corner.

Moisture uptake can have irreversible effects on the mechanical properties of OSB (Wu and Lee 2002; Meza et al 2013). A one-way ANOVA ($\alpha = 0.05$) showed that moisture uptake differed significantly between types 1 and 3 compared with patterns 5 and 6. Tukey's honest significant difference tests showed that wetting patterns 1-3 were associated with high shear wall weight gain and were considered optimal wetting patterns (Ramsey and Schafer 2002). These data were expected because larger wetting patterns should lead to greater moisture retention.

Shear Wall Tests

The shear wall assemblies were able to support a load of 2.44 kN prior to wetting, although removing the uplift corner of the OSB sharply decreased shear wall capacity to 0.99 kN (Table 1). Maximum loads for the dry control assembly group differed significantly from those of the no-corner control assembly group ($p = < 0.001$). This difference illustrates the role of OSB in performance. Maximum loads for wetted assemblies were significantly higher than those for dry control assemblies ($p < 0.001$), but there were no significant differences in maximum loads for the various wetting periods. Although wetting should, intuitively, have a

Table 1. Effect of wetting on maximum load, mass gain, and moisture distribution of simulated shear walls during a 402-da exposure.[a]

Time (da)	Maximum load (kN)	Deflection (mm)	Weight gain (%)	Frequency of moisture distribution pattern types (Fig 3) by assembly (%)					
				1	2	3	4	5	6
0	2.44 (0.20)	19.78 (4.4)	0	—	—	—	—	—	—
0 no corner	0.99 (0.09)	21.97 (2.71)	0	—	—	—	—	—	—
32	3.33 (0.62)	25.23 (7.59)	12.34 (2.54)	12.5	25.0	18.8	0	31.3	12.5
112	3.31 (0.74)	25.06 (7.30)	16.11 (4.91)	31.3	12.5	18.8	25.0	6.3	6.2
177	2.97 (0.40)	28.04 (12.01)	15.08 (3.19)	31.3	31.3	12.5	12.5	6.3	6.3
244	2.79 (0.30)	29.96 (10.29)	16.22 (4.70)	31.3	12.5	12.5	0	37.5	6.3
258	3.09 (0.49)	24.38 (11.07)	15.35 (6.12)	37.5	0	0	0	66.7	12.5
402	2.95 (0.53)		15.18 (3.92)	43.8	12.5	0	0	18.8	25.0

[a] Values represent means of 16 shear wall assemblies per time point except for the 0 time point for which only 8 assemblies were tested. Values in parentheses are standard deviations.

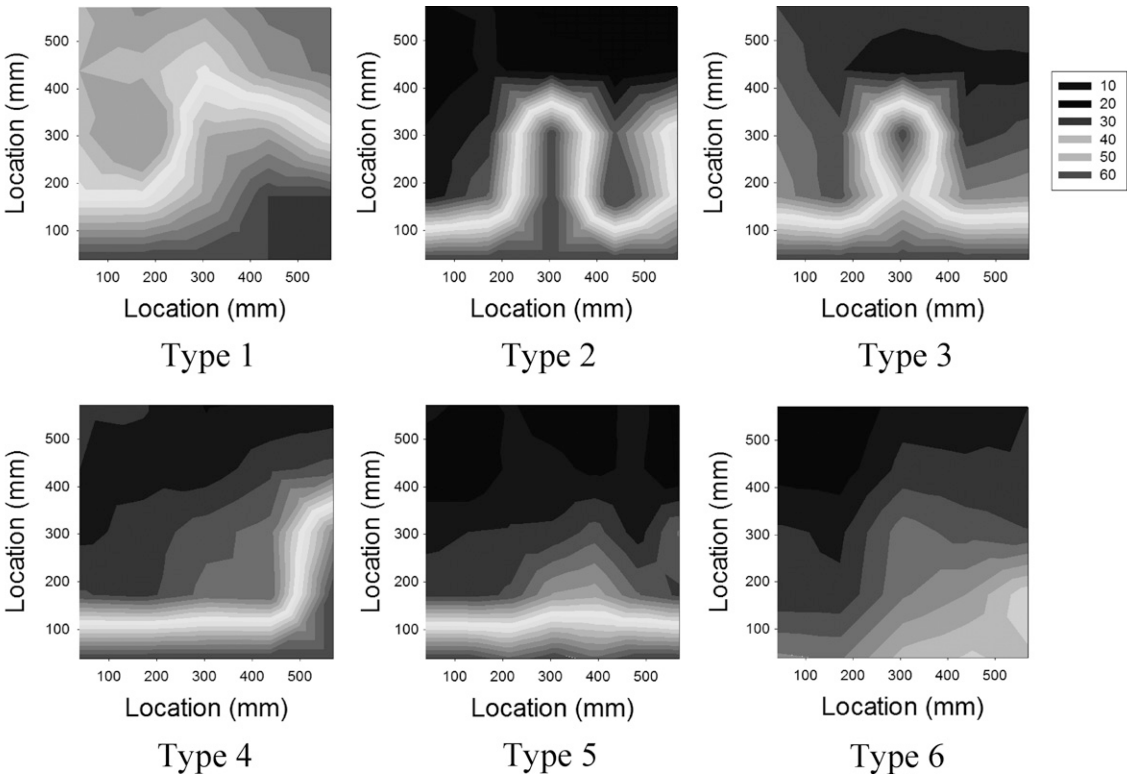

Figure 3. Examples of moisture distribution patterns in shear wall assemblies subjected to regular wetting in the uplift corner (lower right on each diagram) in which lighter colors signify higher moisture levels.

negative effect on capacity, we suspect that the increased capacity was the result of corrosion of the fasteners. Moisture uptake produced a gain in shear wall capacity in the wetted assemblies caused by corrosion in the fasteners from oxidization (Fig 4). The ensuing fastener corrosion increased side friction and led to a stronger connection. Previous studies of preservative-treated wood also suggested that slight corrosion had a positive effect on nail withdrawal resistance (Kang et al 1999). Although this might be beneficial in the short term, continued wetting and corrosion would eventually decrease fastener capacity with a corresponding decrease in shear wall performance.

In addition to changes in overall capacity, the amount of deflection during testing also increased with wetting. Once again, the primary effect occurred after only 32 da of moisture exposure with little noticeable change with additional wet exposure. However, variations in the degree of deflection did increase between 112 and 244 da of exposure, suggesting that prolonged wetting might be beginning to negatively influence the fasteners. Increased deflection after postpeak deflection is not necessarily a negative characteristic because it allows the shear wall to dissipate energy more rapidly. In this case, however, deflection at maximum load increased, signifying decreased capacity. Increased deflection also increased the drift and the likelihood that the wall and the supporting structure would sustain more damage.

Failure modes. Tensile forces in the uplift corner of the shear walls governed failure modes. Nail withdrawal, nail pull-through, flake debonding, and cross-grain tension were the primary failure modes produced by the uplift test

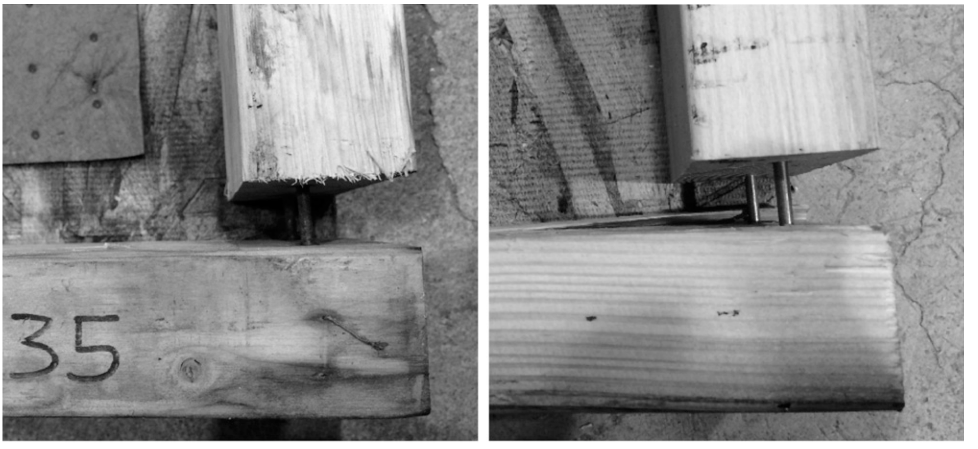

(a) (b)

Figure 4. Examples: (a) wetted assembly with corroded framing nails, (b) dry control shear wall with noncorroded framing nails.

(Fig 5). Nail withdrawal occurred when the applied axial force exceeded the side friction-holding capacity of the nail shaft. The nail then progressively extracted as loads were amplified during testing (Fig 5a-b). Wetting affected OSB rigidity and led to nail pull-through. This failure mode occurred because shear wall loading induced lateral forces on sheathing nails, causing the nail heads to bend and simultaneously crush the OSB (Fig 5c). Flake debonding occurred after nail pull-through, because the sheathing nail heads crushed the OSB, forcing some fragments to separate from the panel (Fig 5c). Cross-grain tension failures occurred when framing nail side friction forces exceeded the radial tension capacity of the dimensional lumber in the sill plate (Fig 5d). Withdrawal occurred in the framing nails in the uplift corner (Fig 5a) and in the sheathing nails along the bottom edge of the OSB paneling in the uplift corner (Fig 5b). This was also observed by Alldritt et al (2014). The sheathing nails along the OSB paneling experienced a combination of bending and side friction failure during loading. Alldritt et al (2014) found that small-scale shear wall strength and stiffness were primarily attributed to the behavior of the connection because OSB panel strength in its original condition vastly exceeded the strength of the connection by a ratio of 15:1. This failure mode was also documented by Foschi (1974). Uplift forces were exerted on the stud and OSB paneling as increasing loads were applied to develop a bending moment on the sheathing nail shafts. The sheathing nails failed simultaneously in bending and withdrawal. Nail heads sunk into the OSB paneling as the shafts of the sheathing nails bent. OSB was able to withstand the sinking force of the nail head in dry control assembly tests but was unable to withstand this force in assemblies subjected to wetting. Strain was greatest in the uplift corner. Thus, sheathing nails closest to the uplift corner experienced the greatest withdrawal and deformation.

The initial failure mode for all shear walls tested was through connections. In some cases, subsequent failures occurred in the OSB and sill plate. Every shear wall tested failed in nail withdrawal. The principal failure mode of the dry control assemblies was nail withdrawal with an occasional cross-grain tensile failure. The principal failure mode for the no-corner control assemblies was also nail withdrawal. Failure modes in the wetted assemblies were governed by nail withdrawal with subsequent failures in nail pull-through. Many of the wetted assemblies also experienced flake debonding, which was occasionally coupled with cross-grain tension.

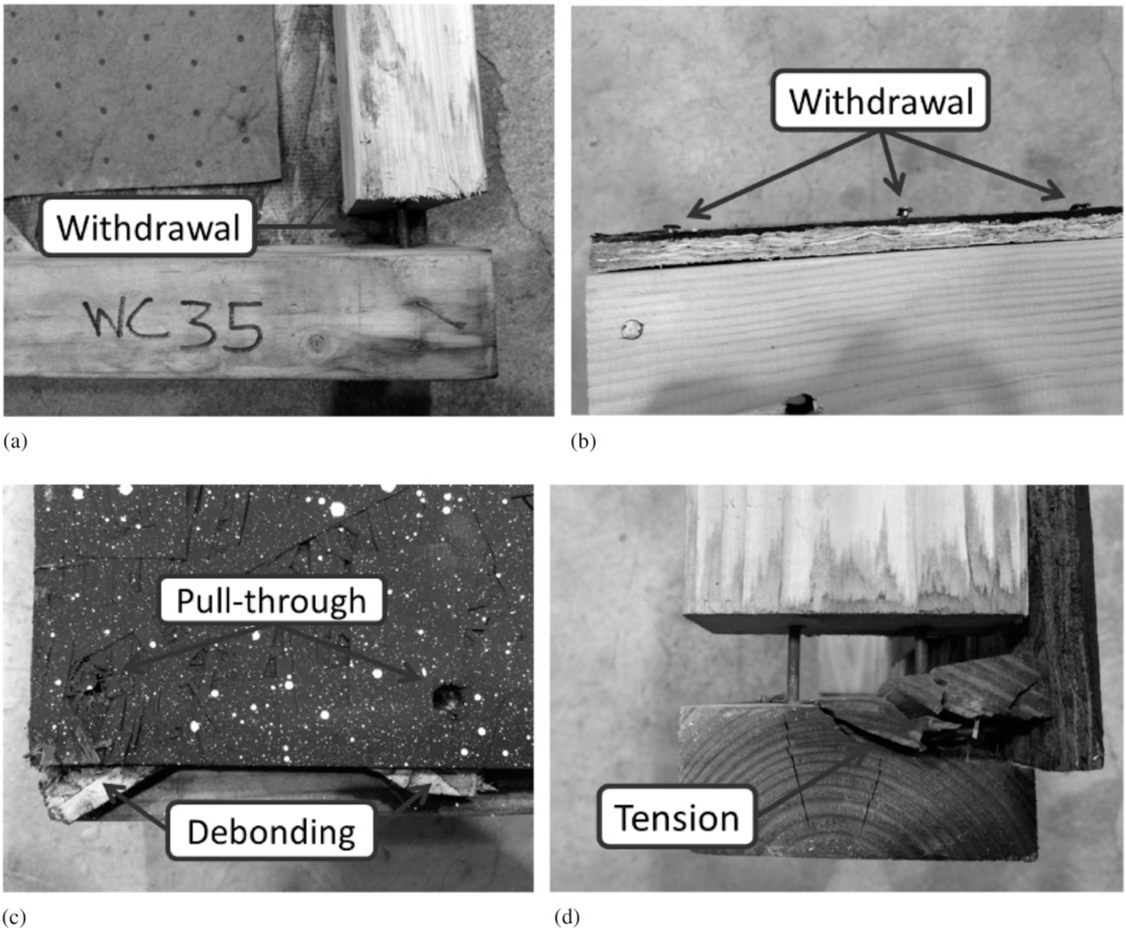

Figure 5. Examples of failure modes in small-scale shear wall assemblies subjected to loading that produced (a) nail withdrawal on the frame in the uplift corner, (b) nail withdrawal on paneling in the uplift corner, (c) nail pull-through and flake debonding on paneling in the uplift corner, and (d) cross-grain tension on the sill plate in the uplift corner of small-scale shear wall assemblies.

The wetted assemblies experienced irreversible moisture effects on OSB mechanical properties that weakened the OSB and caused the sheathing nail heads along the bottom edge of the paneling in the uplift corner to pull through the OSB (Fig 5c). In many cases, the flakes beneath the sheathing nails debonded, causing wood fiber fragmentation (Fig 5c). Sheathing nails along the bottom edge of the dry control assemblies did not fail in this mode (Fig 5b).

Vertical displacement of the sheathing nails in the uplift corner produced tensile failures on the sill plate (Fig 5d). Sheathing nails induced force on the cross grain of the wood in the sill plate as the uplift corner lengthened during loading. In some cases, tensile stress exceeded sill plate capacity depending on grain direction, causing the end grain on the sill plate to split. Tensile failures occurred in dry control, wetted only, and wetted–fungal inoculated assemblies.

Digital image correlation. The DIC data were used to develop contour plots to show progressive strain development during shear wall loading (Fig 6) for a dry control assembly and a wetted assembly. The load cases investigated were 0.50 kN (Fig 6a), 0.94 kN (Fig 6b),

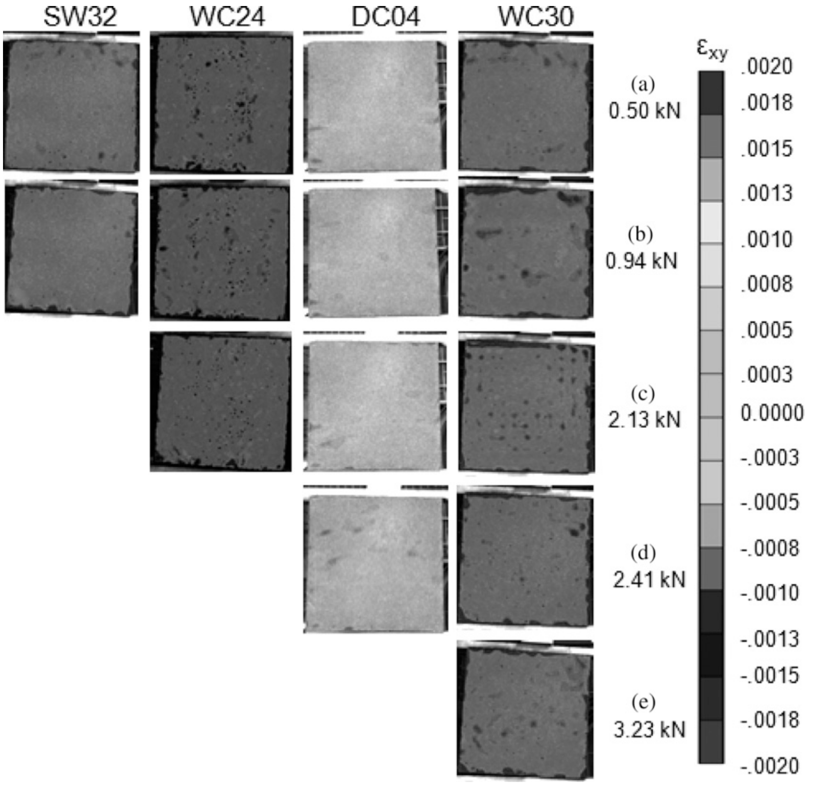

Figure 6. Progressive strain contour plots showing strain in shear walls at (a) 0.50 kN, (b) 0.94 kN, (c) 2.13 kN, (d) 2.41 kN, or (e) 3.23 kN in which the bottom plot in each column represents maximum load (SW, shear wall; WC, water control; DC, control sample).

2.13 kN (Fig 6c), 2.41 kN (Fig 6d), and 3.23 kN (Fig 6e). Contour plots shown at the bottom of each column represent strain in each shear wall just before failure. The level of strain in the contour plots was indicated using a color scale ranging from −0.002 to 0.002. The location of the uplift corner is the lower left corner of each image (Fig 6). Locations of sheathing nails along the sill plate in the uplift corner became evident by the formation of localized strain circles as loads increased (Fig 6).

There was no evidence of strain in reference images of each shear wall. Load was gradually applied, and subsequent images were compared. Small amounts of strain, albeit small in magnitude, began to develop around the corner sheathing nail in the uplift corner of each shear wall at a load of 0.50 kN (Fig 6a), but there were no discernible differences among shear wall groups at this load.

Dry control and wetted assemblies showed strain development on the corner sheathing nail in the uplift corner (Fig 6b), and then strain circles developed along the sill plate in the uplift corner at a load of 2.13 kN (Fig 6c). There were no discernible differences between the dry and wetted assemblies as load was applied beyond 2.13 kN (Fig 6d-e). There were constant strain circles around the sheathing nail heads along the sill plate in the uplift corner. In some cases, the corner sheathing nail in the uplift corner would experience a drop in strain caused by cross-grain failure in the sill plate.

The majority of the OSB panels sustained very little strain in the uplift tests. This supports the observation that failure occurred at the connections.

CONCLUSIONS

Although it was difficult to reliably develop fungal attack in the shear wall assemblies under the conditions used, wetting alone initially increased shear wall capacity, possibly as a result of small amounts of fastener corrosion. However, prolonged wetting altered the failure modes of the assemblies, and continued moisture exposure eventually diminished fastener capacity to the point at which the system did not perform as designed. These results suggest that limited wetting affected the OSB and the failure mode of shear walls but was not detrimental with respect to load capacity. These results suggest the need for further studies on the effects of prolonged wetting on performance.

ACKNOWLEDGMENTS

The authors extend their deepest gratitude to the USDA Center for Wood Utilization Research for supporting this work. The authors also thank Milo Clauson and Camille Freitag, Senior Faculty Research Assistants, for their valuable feedback and technical assistance. The authors also acknowledge the assistance of Byrne T. Miyamoto, undergraduate student.

REFERENCES

Alldritt K, Sinha A, Miller TH (2014) Designing a strand orientation pattern for improved shear properties of oriented strand board. J Mater Civil Eng 26(7):04014022-1-0401422-9.

ASTM (2012) E564. Standard practice for static load test for shear resistance of framed walls for buildings. American Society for Testing and Materials, West Conshohocken, PA.

Chui YH, Ni C, Jiang L (1998) Finite-element model for nailed wood joints under reversed cyclic load. J Struct Eng 124(1):96-103.

Durham J, Lam F, Prion HG (2001) Seismic resistance of wood shear walls with large OSB panels. J Struct Eng 127(12):1460-1466.

Foschi RO (1974) Load-slip characteristics of nails. J Wood Sci 7(1):69-74.

Johnson AC (1997) Monotonic and cyclic performance of long shear walls with openings. MS thesis, Virginia Polytechnic Institute and State University, Blacksburg, VA.

Kang SM, Morrell JJ, Smith D (1999) Effect of incising and preservative treatment on nail-holding capacity of Douglas-fir and hem-fir lumber. Forest Prod J 49(3): 43-45.

Kent SM, Leichti RJ, Rosowsky DV, Morrell JJ (2004) Effects of decay by *Postia placenta* on the lateral capacity of nailed oriented strandboard sheathing and Douglas-fir framing members. Wood Fiber Sci 36(4):560-572.

Kent SM, Leichti RJ, Rosowsky DV, Morrell JJ (2005) Effects of decay on cyclic properties of nailed connections. J Mater Civil Eng 17(5):579-585.

McCutcheon WJ (1985) Racking deformations in wood shear walls. J Struct Eng 111(2):257-269.

Meza L, Sinha A, Morrell JJ (2013) Effect of wetting during construction on properties of Douglas-fir plywood and oriented strandboard flooring. Forest Prod J 63(5/6): 199-201.

NDS (2012) National design specification for wood construction. American Forest and Paper Association, Inc., Washington, DC.

Polensek A, Bastendorff KM (1987) Damping in nailed joints of light-frame wood buildings. Wood Fiber Sci 19(2):110-125.

Ramsey FL, Schafer DW (2002) The statistical sleuth: A course in methods of data analysis. Cengage Learning, Stamford, CT. 768 pp.

Sinha A, Gupta R (2009) Strain distribution in OSB and GWB in wood-frame shear walls. J Struct Eng 135(6): 666-675.

van de Lindt JW (2004) Evolution of wood shear wall testing, modeling, and reliability analysis: Bibliography. Pract Period Struct Des Constr 9(1):44-53.

Wu Q, Lee JN (2002) Thickness swelling of oriented strandboard under long-term cyclic humidity exposure condition. Wood Fiber Sci 34(1):125-139.